The effect of the energy functional on the pasta-phase properties of catalysed neutron stars

Hoa DINH THI, Anthea FANTINA, Francesca GULMINELLI

November 25, 2021

International Worshop on Multi-facets of EOS and Clustering

UNIVERSITÉ CAEN NORMANDIE

GANIL laboratoire commun CEA/DRF spiral2 CNRS/IN2P3

lpc caen laboratoire de physique corpusculaire

1. Pasta phase in neutrons stars

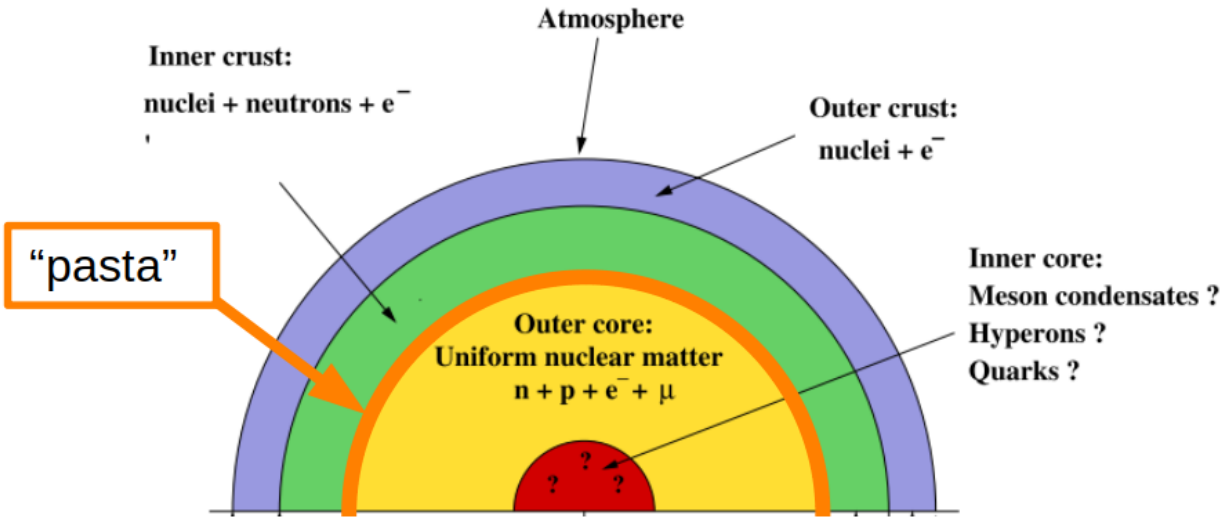

→ **Pasta phase** is expected to exist at the bottom of the **inner crust**, before the transition to the **core**.

Original figure taken from Fiorella Burgio, G.; Vidana, I. Universe 2020, 6(8), 119

2. Different shapes in the pasta phase

- 5 phases: spheres, rods, slabs, $\underbrace{\text{tubes, bubbles}}_{\text{“inverted” configurations}}$

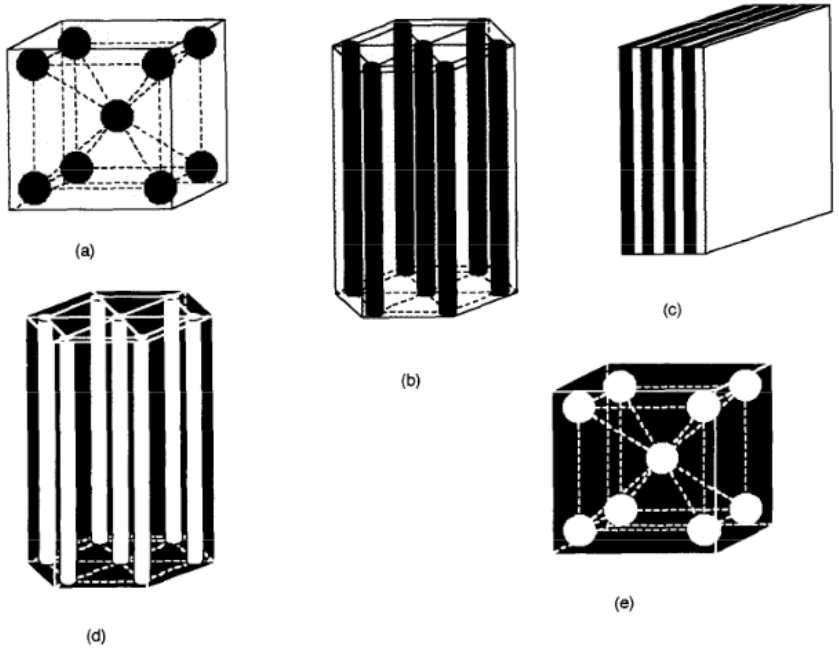

Ravenhall et al., Phys. Rev. Lett. 27, 2066 (1983)
Hashimoto et al., Prog. Theor. Phys. 71, 320 (1984)
K. Oyamatsu, Nucl. Phys. A561, 431 (1993)

3. Formalism

Thermodynamic potential in a **C**ompressible **L**iquid **D**rop **M**odel:

$$\begin{aligned}\Omega &= n_p m_p c^2 + (n_B - n_p) m_n c^2 \\ &+ n_0 e_{HM}(n_0, I)\mathsf{f} + \epsilon_{surf} + \epsilon_{curv} + \epsilon_{Coul} \\ &+ n_g e_{HM}(n_g, 1)(1 - \mathsf{f}) + \epsilon_e - \mu n_B.\end{aligned}$$

3. Formalism

Thermodynamic potential in a **C**ompressible **L**iquid **D**rop **M**odel:

$$\Omega = n_p m_p c^2 + (n_B - n_p) m_n c^2$$
$$+ n_0 e_{HM}(n_0, I)\mathsf{f} + \epsilon_{surf} + \epsilon_{curv} + \epsilon_{Coul}$$
$$+ n_g e_{HM}(n_g, 1)(1 - \mathsf{f}) + \epsilon_e - \mu n_B.$$

3. Formalism

Thermodynamic potential in a **C**ompressible **L**iquid **D**rop **M**odel:

$$\Omega = n_p m_p c^2 + (n_B - n_p) m_n c^2$$
$$+ \; n_0 e_{HM}(n_0, I)\mathsf{f} + \epsilon_{surf} + \epsilon_{curv} + \epsilon_{Coul}$$
$$+ n_g e_{HM}(n_g, 1)(1 - \mathsf{f}) + \epsilon_e - \mu n_B.$$

3. Formalism

Thermodynamic potential in a **C**ompressible **L**iquid **D**rop **M**odel:

$$\begin{aligned}\Omega &= n_p m_p c^2 + (n_B - n_p) m_n c^2 \\ &+ n_0 e_{HM}(n_0, I)\mathsf{f} + \epsilon_{surf} + \epsilon_{curv} + \epsilon_{Coul} \\ &+ n_g e_{HM}(n_g, 1)(1 - \mathsf{f}) + \epsilon_e - \mu n_B.\end{aligned}$$

3. Formalism

Thermodynamic potential in a **C**ompressible **L**iquid **D**rop **M**odel:

$$\begin{aligned}\Omega &= n_p m_p c^2 + (n_B - n_p) m_n c^2 \\ &+ n_0 e_{HM}(n_0, I)\mathsf{f} + \epsilon_{surf} + \epsilon_{curv} + \epsilon_{Coul} \\ &+ n_g e_{HM}(n_g, 1)(1 - \mathsf{f}) + \epsilon_e - \mu n_B \,.\end{aligned}$$

3. Formalism

Thermodynamic potential in a **C**ompressible **L**iquid **D**rop **M**odel:

$$\Omega = n_p m_p c^2 + (n_B - n_p) m_n c^2$$
$$+ n_0 \, e_{HM}(n_0, I) \, \mathsf{f} + \epsilon_{surf} + \epsilon_{curv} + \epsilon_{Coul}$$
$$+ n_g e_{HM}(n_g, 1)(1 - \mathsf{f}) + \epsilon_e - \mu n_B .$$

- Bulk energy, $e_{HM}(n, \delta))$, is calculated using the **meta-modeling** technique.

3. Formalism

Thermodynamic potential in a **C**ompressible **L**iquid **D**rop **M**odel:

$$\Omega = n_p m_p c^2 + (n_B - n_p) m_n c^2$$
$$+ n_0 \, e_{HM}(n_0, I) \, \mathsf{f} + \epsilon_{surf} + \epsilon_{curv} + \epsilon_{Coul}$$
$$+ n_g e_{HM}(n_g, 1)(1 - \mathsf{f}) + \epsilon_e - \mu n_B .$$

- Bulk energy, $e_{HM}(n, \delta))$, is calculated using the **meta-modeling** technique.
  $\rightarrow$ 13 **bulk** parameters: $E_{sat/sym}$, n_{sat}, L_{sym}, $K_{sat/sym}$, ...
  Margueron et al. Phys. Rev. C, 97:025806, 2018

3. Formalism

Thermodynamic potential in a **C**ompressible **L**iquid **D**rop **M**odel:

$$\Omega = n_p m_p c^2 + (n_B - n_p) m_n c^2$$
$$+ n_0 \, e_{HM}(n_0, I) \, \mathsf{f} + \epsilon_{surf} + \epsilon_{curv} + \epsilon_{Coul}$$
$$+ n_g e_{HM}(n_g, 1)(1 - \mathsf{f}) + \epsilon_e - \mu n_B.$$

- Bulk energy, $e_{HM}(n, \delta))$, is calculated using the **meta-modeling** technique.
  $\rightarrow$ 13 **bulk** parameters: $E_{sat/sym}$, n_{sat}, L_{sym}, $K_{sat/sym}$, ...
  Margueron et al. Phys. Rev. C, 97:025806, 2018
- Surface, curvature, and Coulomb energies depend on nuclear shape. $\rightarrow$ 5 surface parameters: σ_0, $\sigma_{0,c}$, β, b_s, p

Equilibrium configuration

- **Step 1**: Minimizing Ω for each geometry

Equilibrium configuration

- **Step 1**: Minimizing Ω for each geometry
  $\rightarrow$ composition (n_p, I, n_0, n_g, r_N)

Equilibrium configuration

- **Step 1**: Minimizing Ω for each geometry
  $\rightarrow$ composition (n_p, I, n_0, n_g, r_N) + energy density.

Equilibrium configuration

- **Step 1**: Minimizing Ω for each geometry
  $\rightarrow$ composition (n_p, I, n_0, n_g, r_N) + energy density.
- **Step 2**: Comparing energy densities among all geometries
  $\rightarrow$ equilibrium geometry.

4. Model dependence of pasta-phase properties

Equilibrium geometries

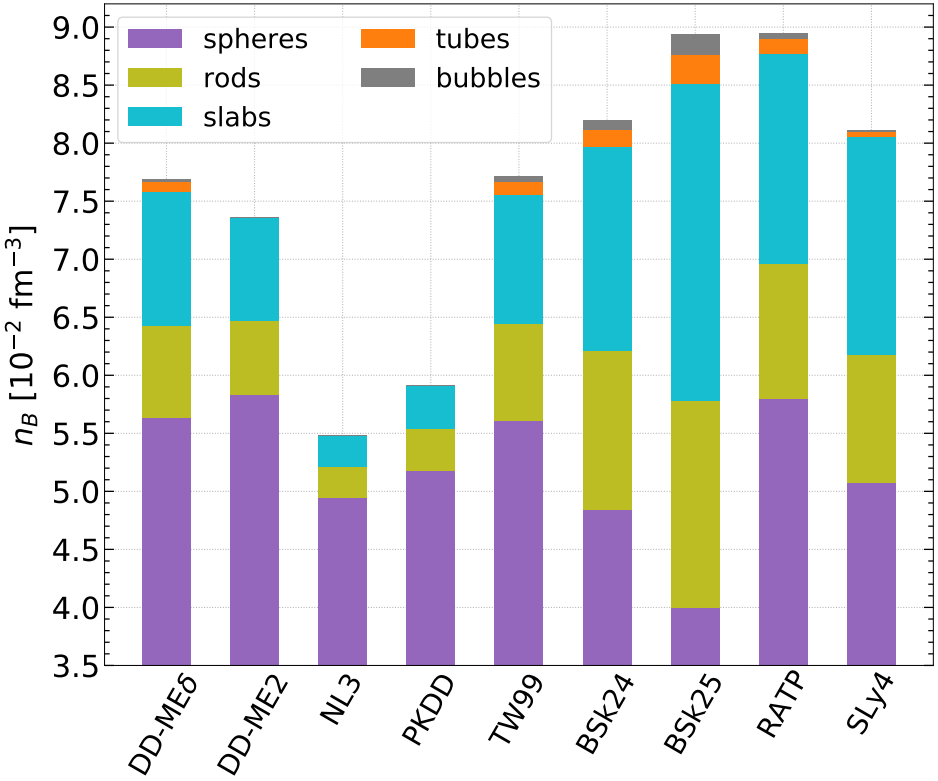

4. Model dependence of pasta-phase properties

Equilibrium geometries

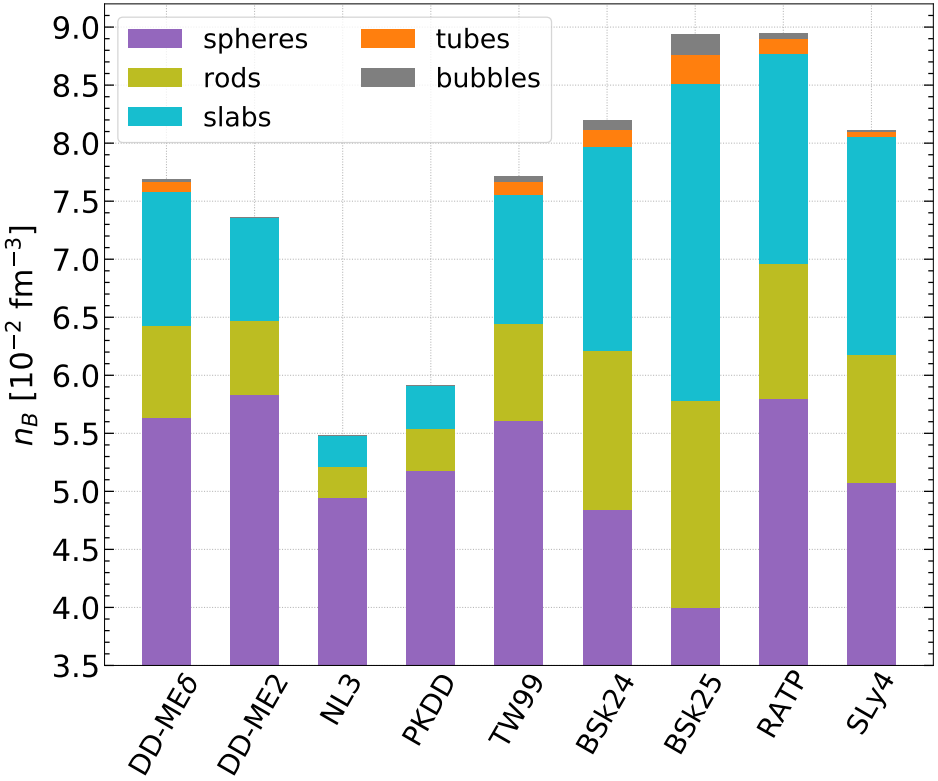

Proton fraction $y_p = Z/A$

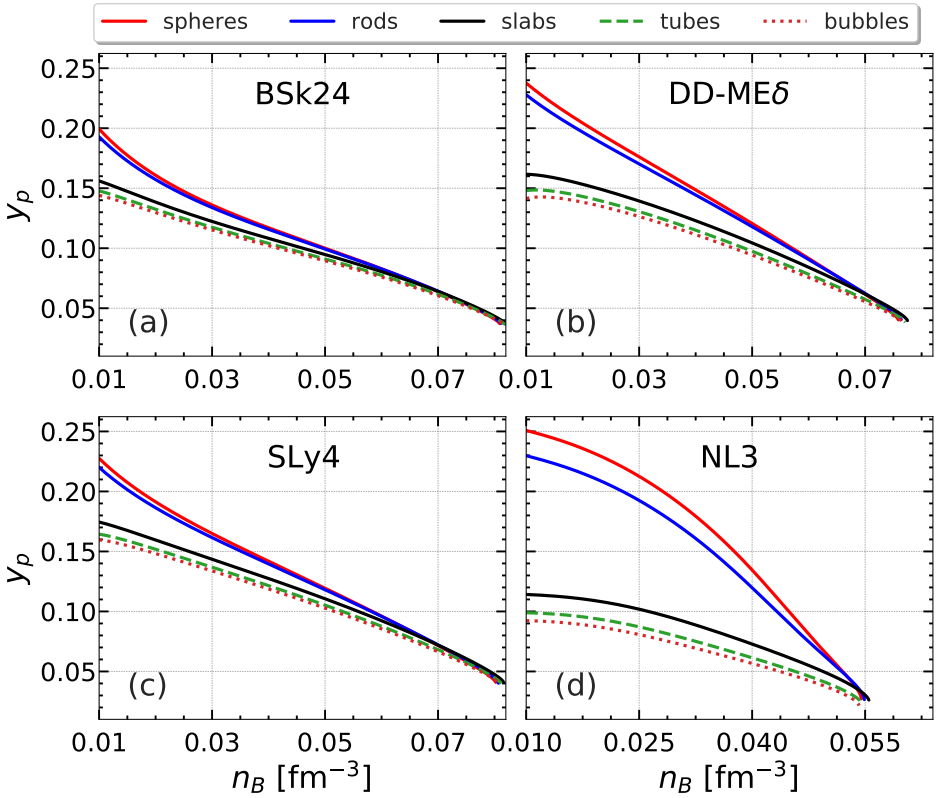

4. Model dependence of pasta-phase properties

Equilibrium geometries

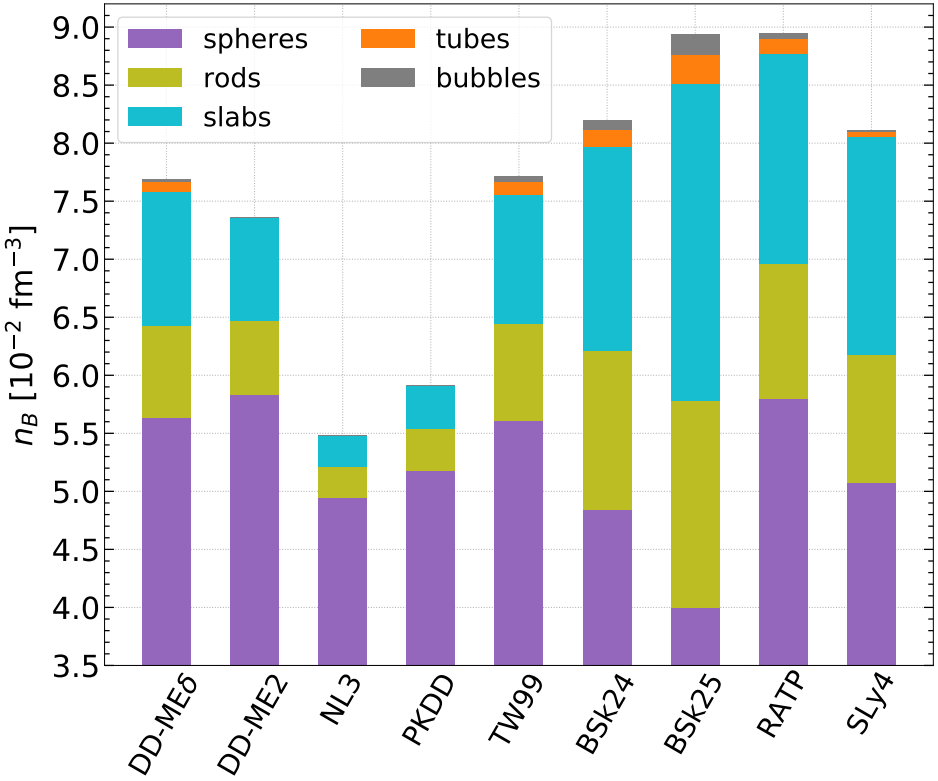

Proton fraction $y_p = Z/A$

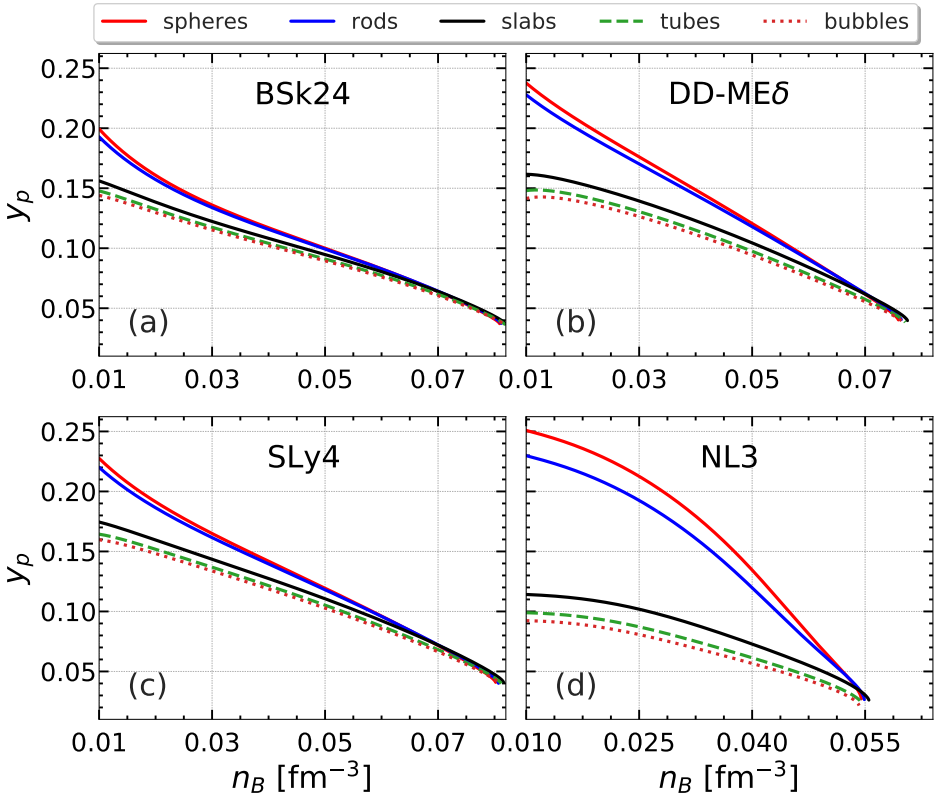

- Properties of pasta phases are model dependent.

4. Model dependence of pasta-phase properties

Equilibrium geometries

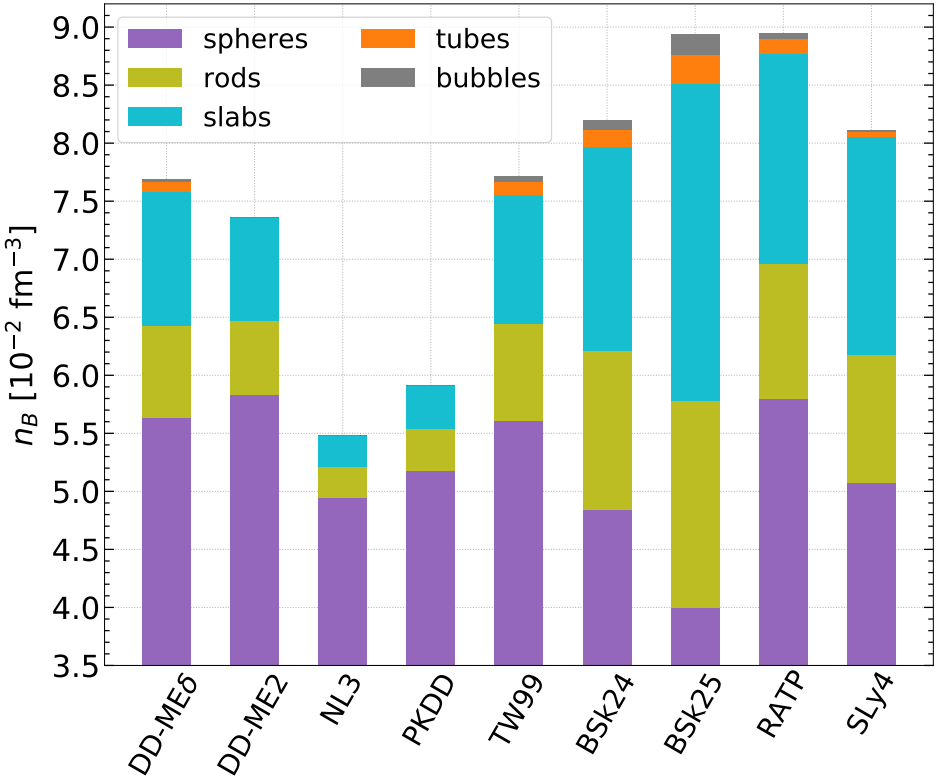

Proton fraction $y_p = Z/A$

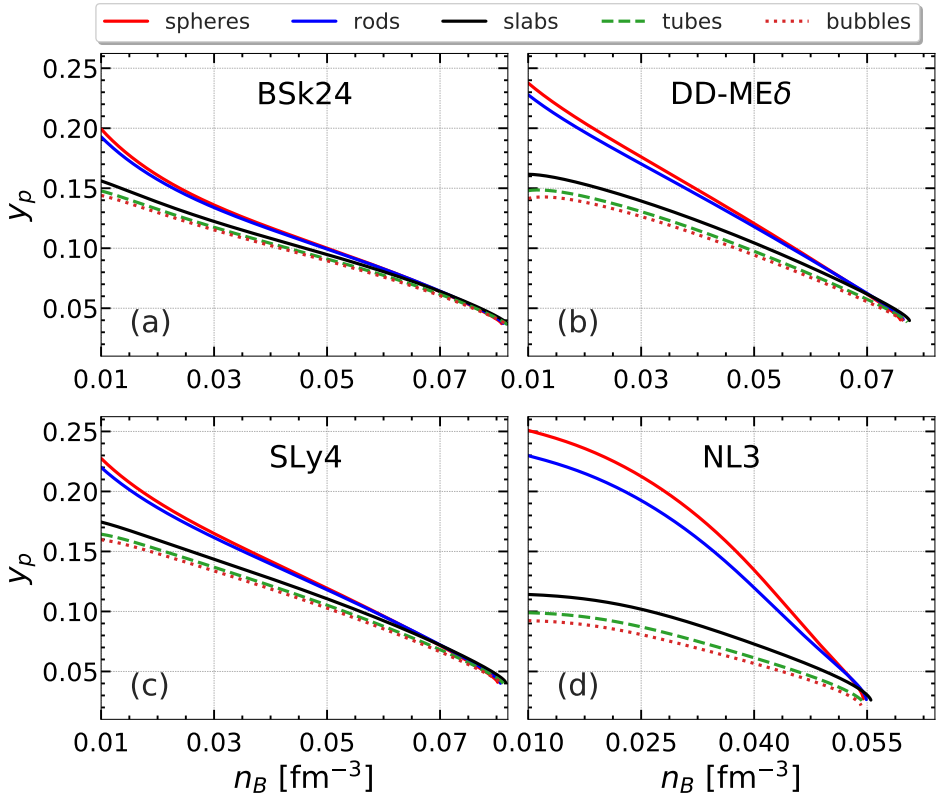

- Properties of pasta phases are model dependent.
- Use Bayesian analysis to study the influence of energy functional on the uncertainties of pasta-phase properties.

Dinh Thi, H., et al. . Eur. Phys. J. A 57, 296 (2021)

5. Bayesian analysis

- Prior distribution: generated based on the current nuclear physics knowledge. (See Margueron et al. Phys. Rev. C, 97:025806, 2018)

5. Bayesian analysis

- Prior distribution: generated based on the current nuclear physics knowledge. (See Margueron et al. Phys. Rev. C, 97:025806, 2018)
- Posterior distribution: obtained by applying 2 constraints on the prior.

5. Bayesian analysis

- Prior distribution: generated based on the current nuclear physics knowledge. (See Margueron et al. Phys. Rev. C, 97:025806, 2018)
- Posterior distribution: obtained by applying 2 constraints on the prior.

1. Low density (LD) filter (Drischler et al., Phys. Rev. C, 93, 054314, 2016):

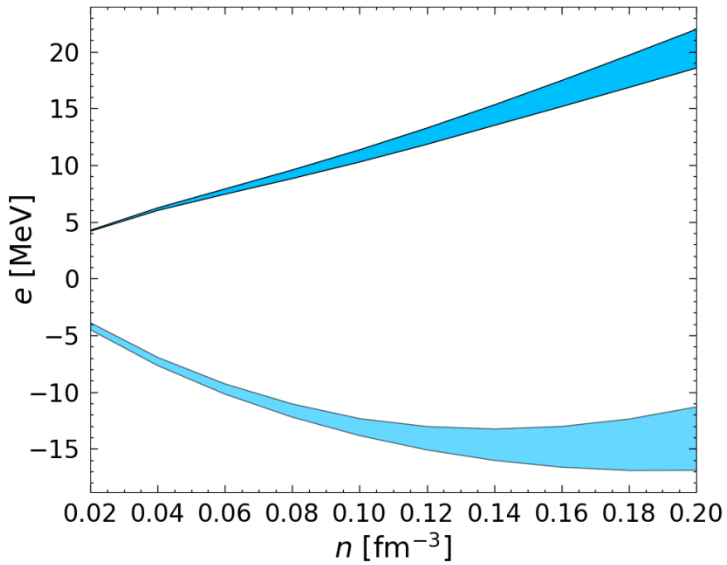

5. Bayesian analysis

- Prior distribution: generated based on the current nuclear physics knowledge. (See Margueron et al. Phys. Rev. C, 97:025806, 2018)
- Posterior distribution: obtained by applying 2 constraints on the prior.

1. Low density (LD) filter (Drischler et al., Phys. Rev. C, 93, 054314, 2016):

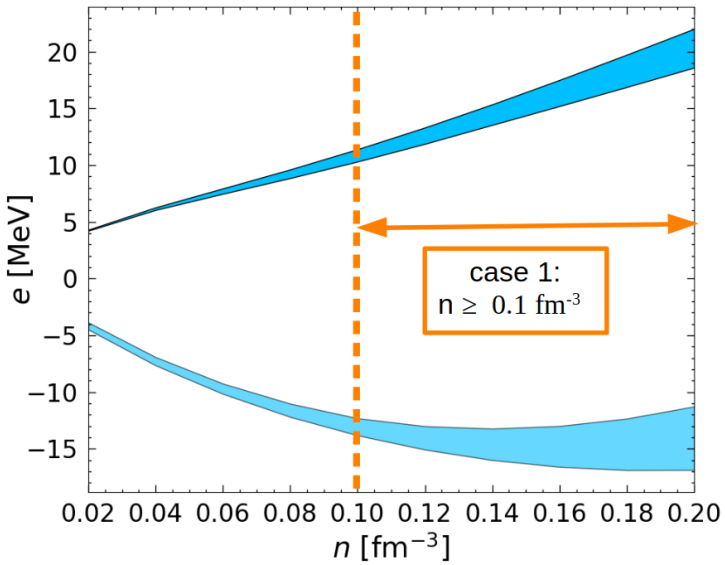

5. Bayesian analysis

- Prior distribution: generated based on the current nuclear physics knowledge. (See Margueron et al. Phys. Rev. C, 97:025806, 2018)
- Posterior distribution: obtained by applying 2 constraints on the prior.

1. Low density (LD) filter (Drischler et al., Phys. Rev. C, 93, 054314, 2016):

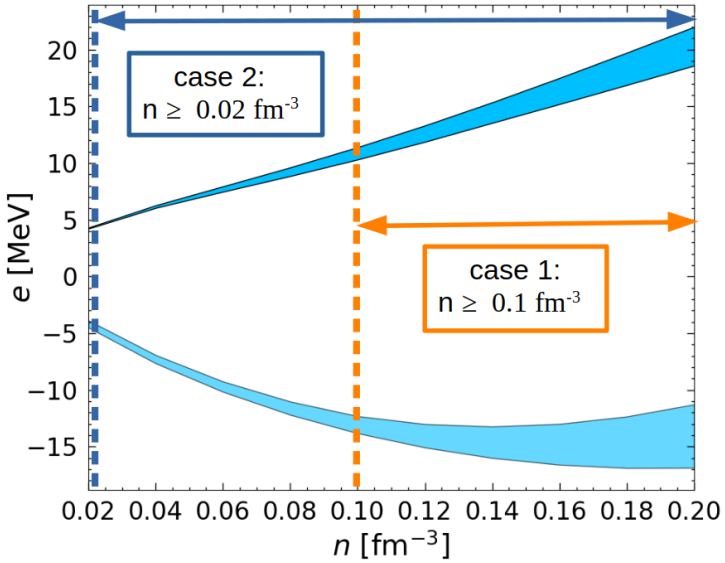

5. Bayesian analysis

- Prior distribution: generated based on the current nuclear physics knowledge. (See Margueron et al. Phys. Rev. C, 97:025806, 2018)
- Posterior distribution: obtained by applying 2 constraints on the prior.

1. Low density (LD) filter (Drischler et al., Phys. Rev. C, 93, 054314, 2016):

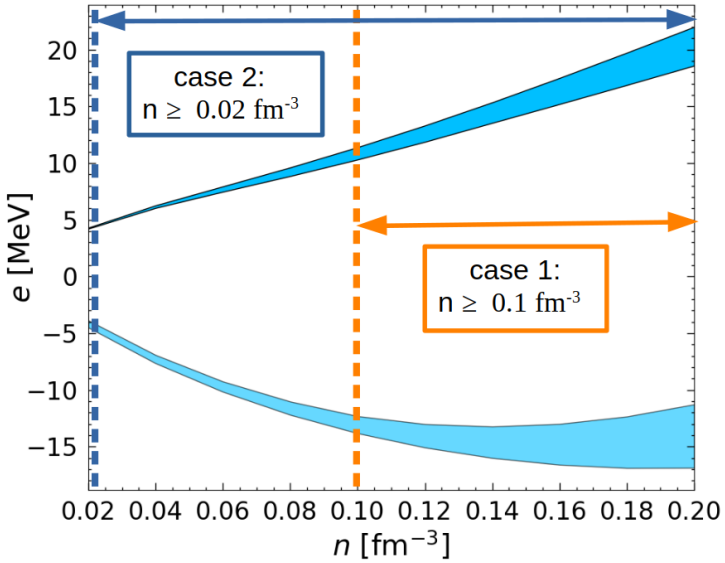

2. High density (HD) filter: $c_s/c < 1$; $dP/d\rho > 0$; $e_{sym} \geq 0$; and $M_{max} \geq 1.97 M_\odot$.

5.1. Compatibility of the posterior and observations

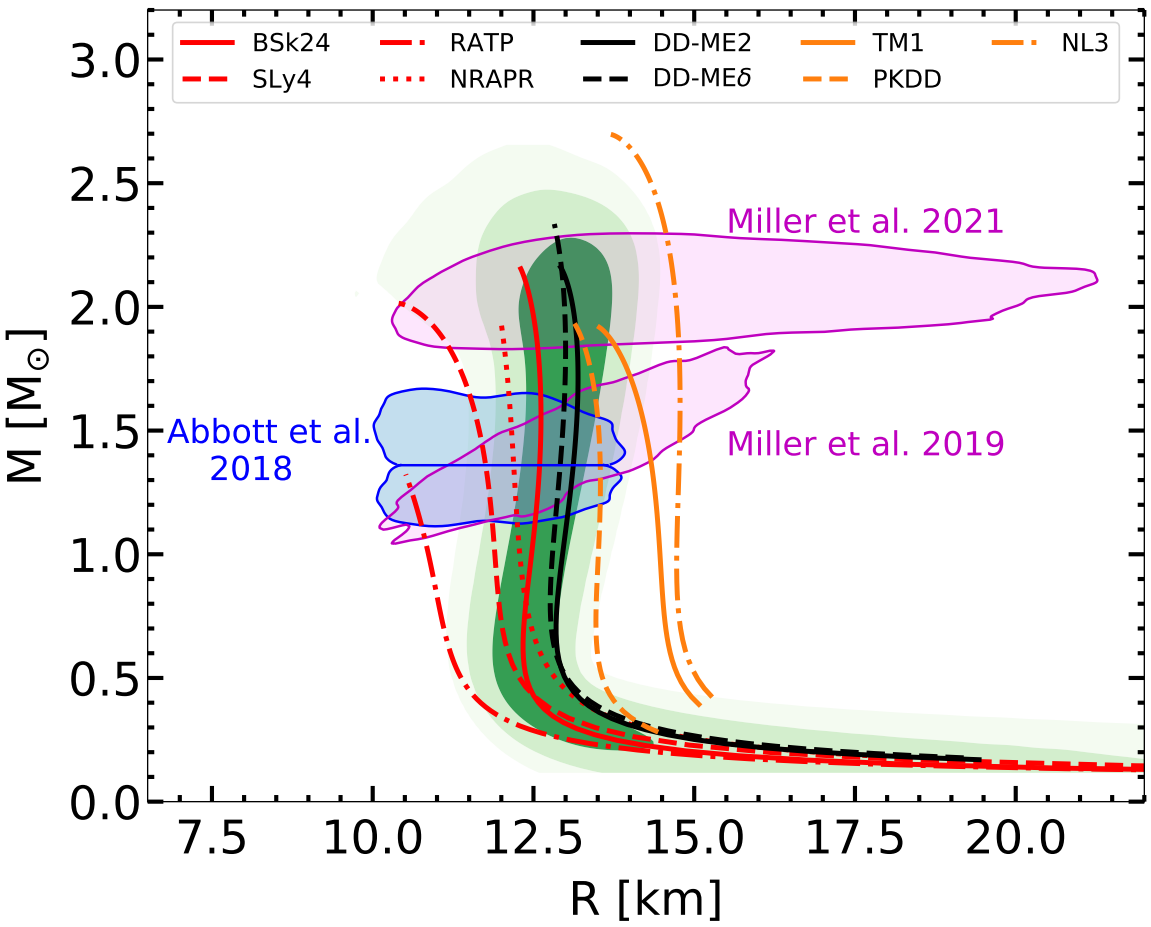

H. Dinh Thi et al. A&A 654, A114 (2021)

→ Posterior M-R distribution is in good agreement with results from NICER and LIGO/Virgo.

5.2. Uncertainties in pasta-phase properties

Sphere-pasta transition:

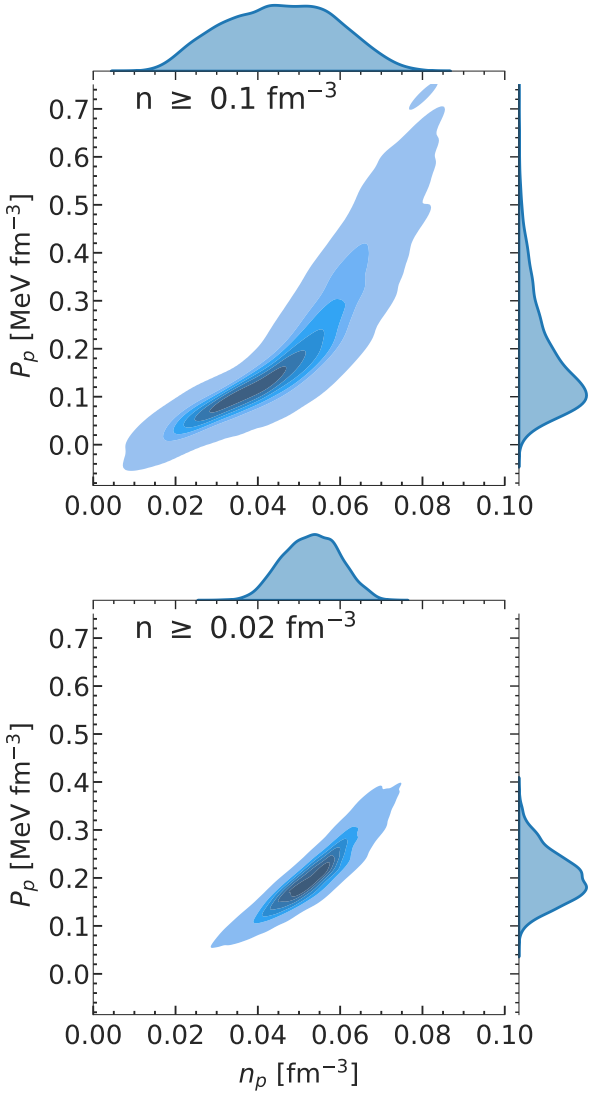

5.2. Uncertainties in pasta-phase properties

Sphere-pasta transition:

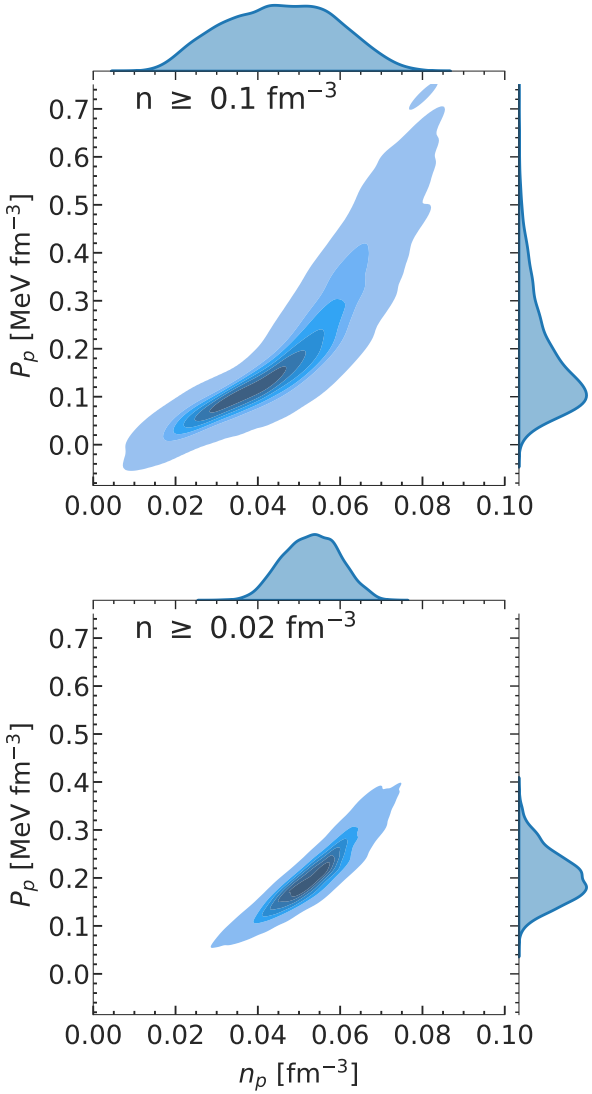

Dinh Thi, H., et al. . Eur. Phys. J. A 57, 296 (2021);

Thickness&moment of inertia:

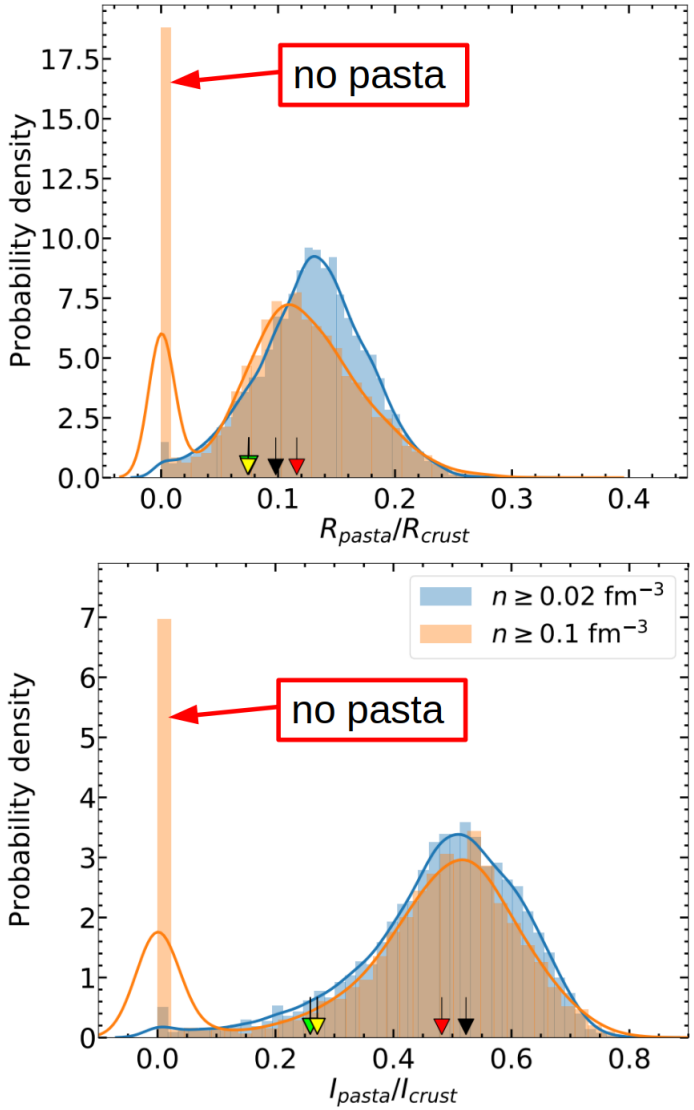

H. Dinh Thi et al. A&A 654, A114 (2021)

5.3. Crust-core transition density

H. Dinh Thi et al. A&A 654, A114 (2021)

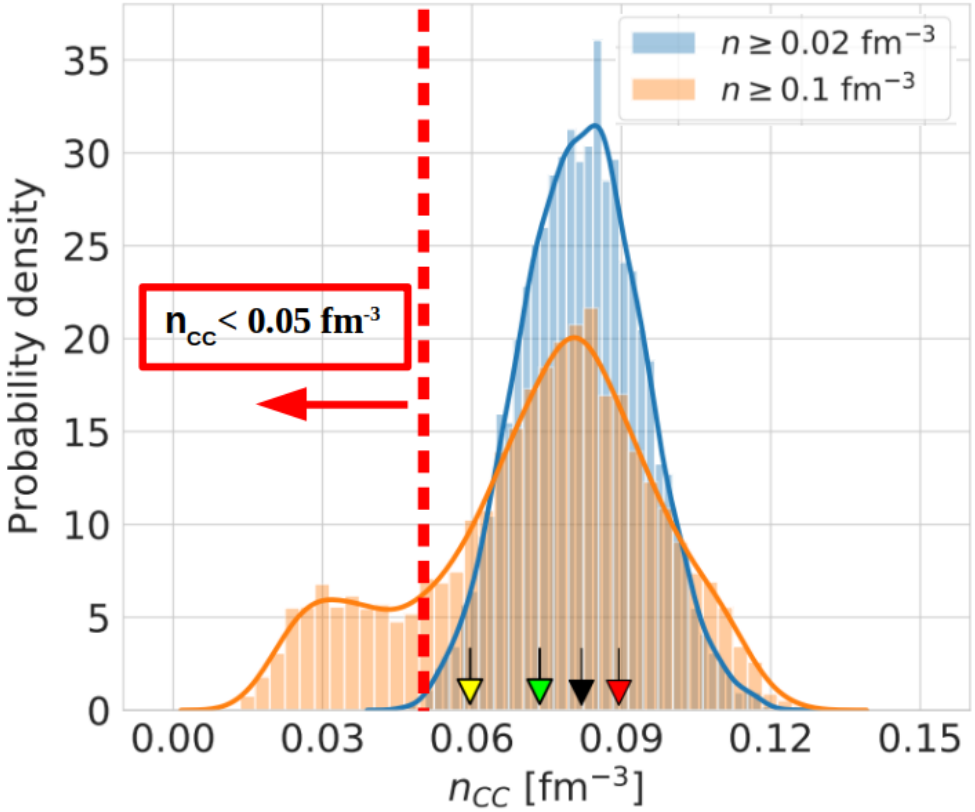

- Models resulting in $n_{CC} < 0.05$ fm^{-3} are eliminated if the LD filter is applied from 0.02 fm^{-3}.

5.4. Nuclear matter energy

Dinh Thi, H., et al. . Eur. Phys. J. A 57, 296 (2021)

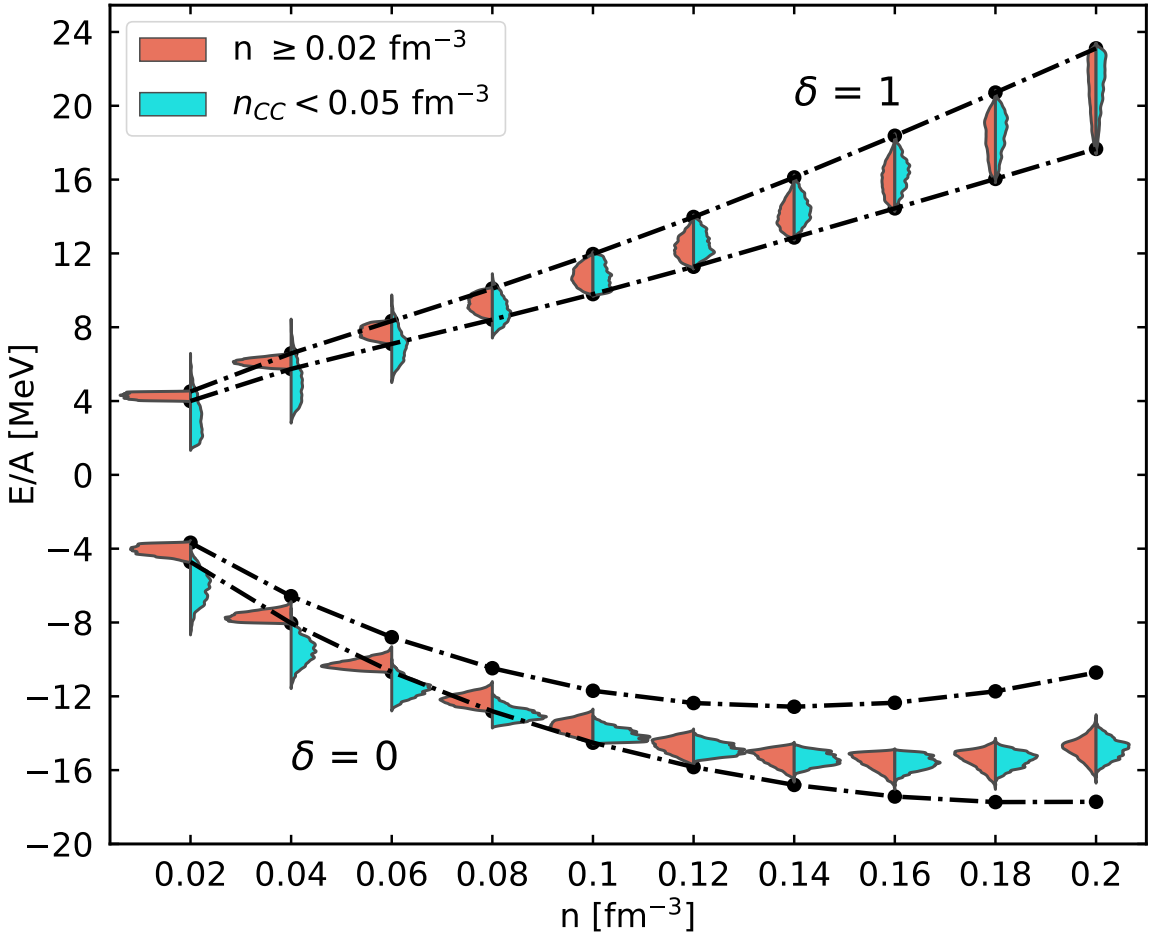

- Models satisfying the LD filter at n $\geq$ 0.1 fm^{-3} and associated $n_{CC} < 0.05$ fm^{-3} result in lower E/A at density n $<$ 0.1 fm^{-3}.

5.5. Equation of state

H. Dinh Thi et al. A&A 654, A114 (2021)

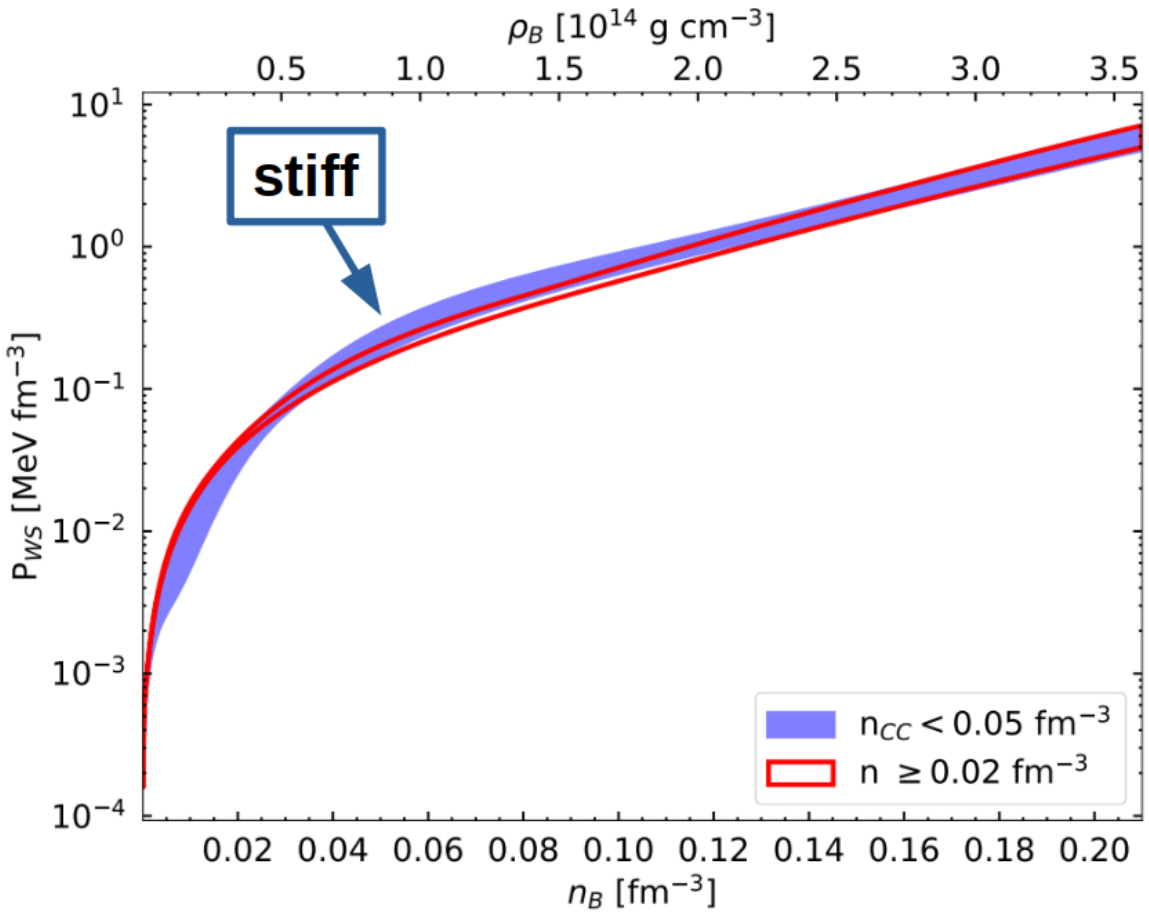

- Models satisfying the LD filter at n $\geq$ 0.1 fm^{-3} and associated $n_{CC} < 0.05$ fm^{-3} result in stiffer EoS at density n $<$ 0.1 fm^{-3}.

5.6. Empirical parameters

Isoscalar parameters

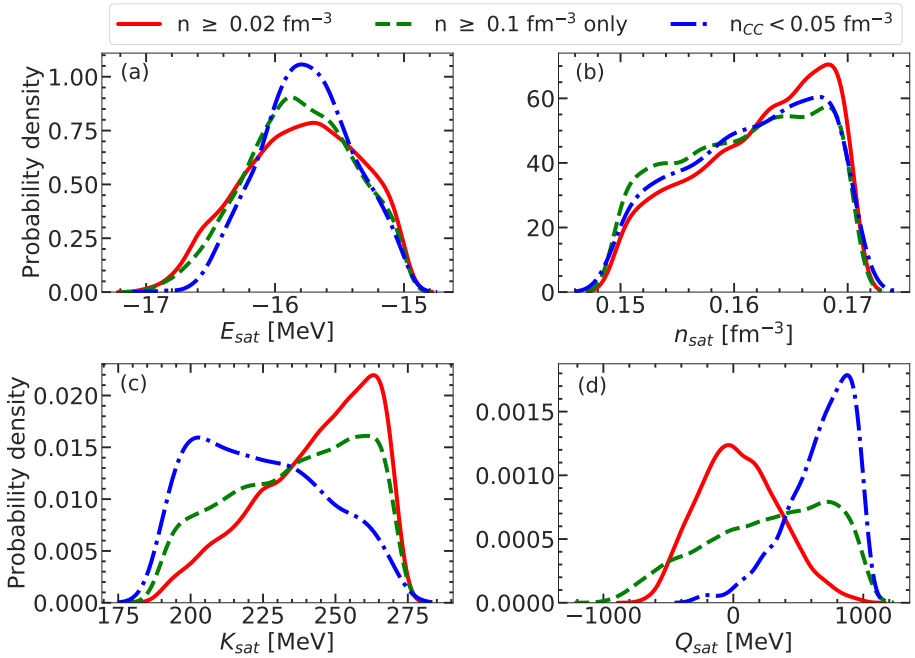

Isovector parameters

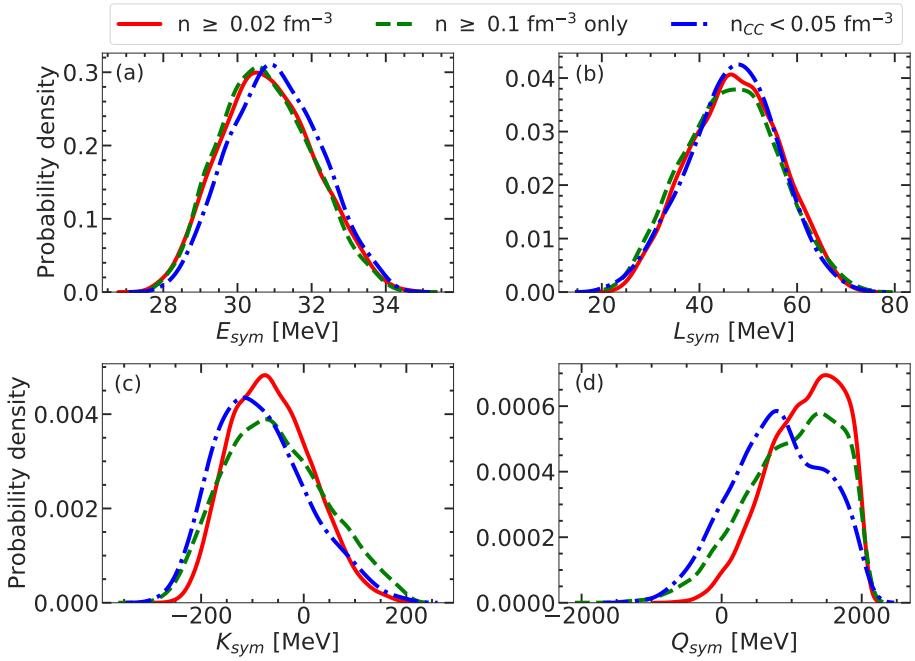

5.6. Empirical parameters

Isoscalar parameters

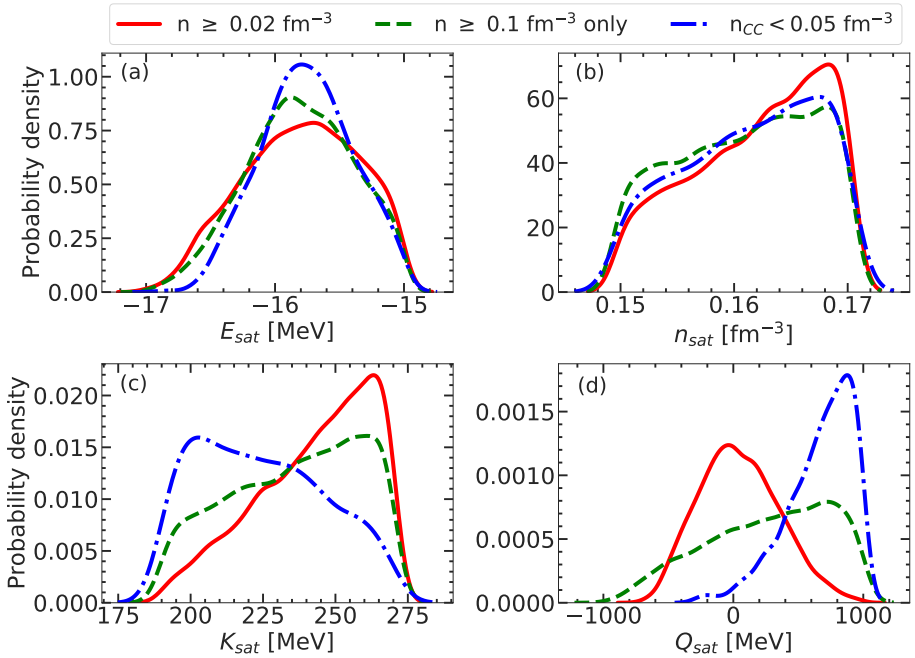

Isovector parameters

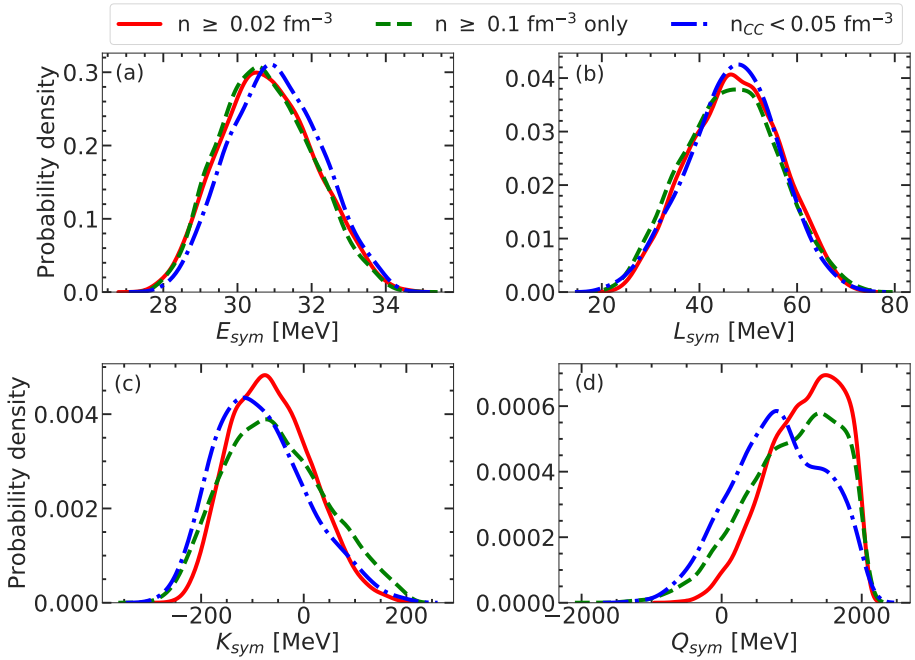

- Taylor expansions ($x = \dfrac{n - n_{sat}}{3n_{sat}}$, where $n_{sat} \approx 0.15$ fm^{-3}):

$$e(n,\delta) \approx E_{\rm sat} + \frac{1}{2} K_{\rm sat} x^2 + \frac{1}{6} Q_{\rm sat} x^3 + \delta^2 \left(E_{\rm sym} + L_{\rm sym} x + \frac{1}{2} K_{\rm sym} x^2 + \frac{1}{6} Q_{\rm sym} x^3 \right) ,$$

$$P(n,\delta) \approx \frac{n_{\rm sat}}{3} (1+3x)^2 \left[K_{\rm sat} x + \frac{1}{2} Q_{\rm sat} x^2 + \delta^2 \left(L_{\rm sym} + K_{\rm sym} x + \frac{1}{2} Q_{\rm sym} x^2 \right) \right] .$$

5.6. Empirical parameters

Isoscalar parameters

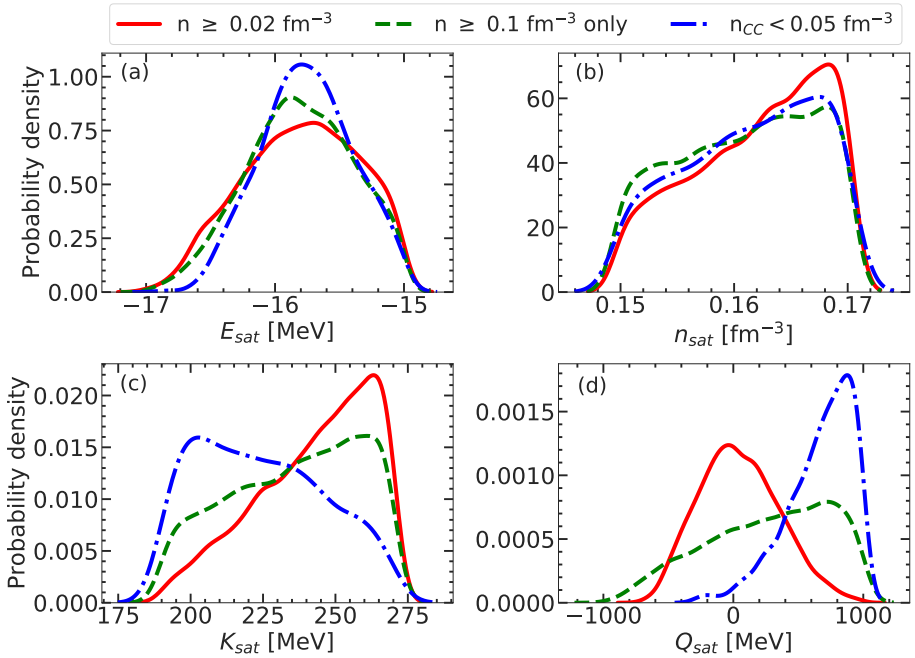

Isovector parameters

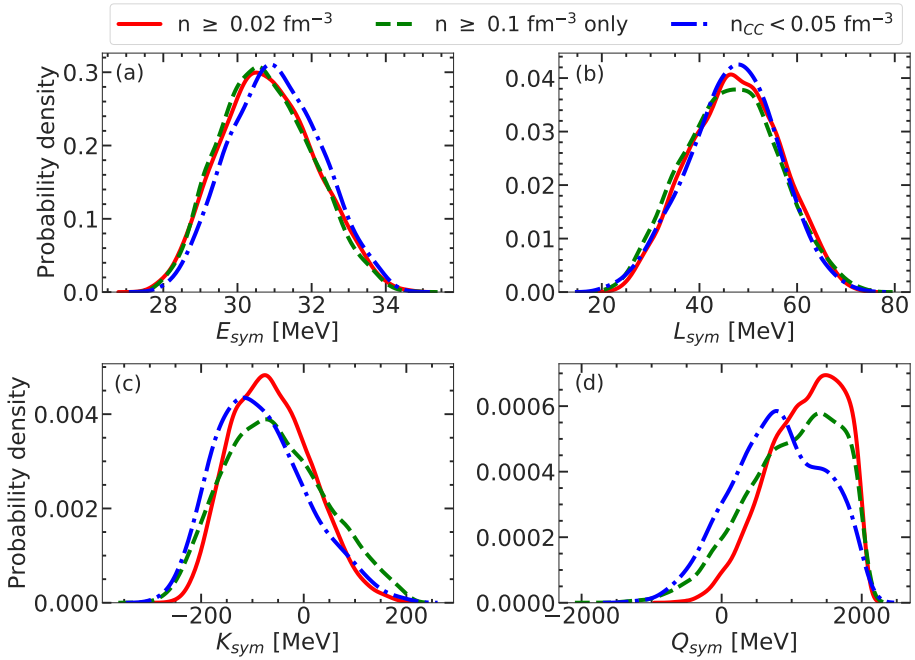

- Taylor expansions ($x = \dfrac{n - n_{sat}}{3n_{sat}}$, where $n_{sat} \approx 0.15$ fm^{-3}):

$$e(n,\delta) \approx E_{\rm sat} + \frac{1}{2} K_{\rm sat} x^2 + \frac{1}{6} Q_{\rm sat} x^3 + \delta^2 \left(E_{\rm sym} + L_{\rm sym} x + \frac{1}{2} K_{\rm sym} x^2 + \frac{1}{6} Q_{\rm sym} x^3 \right) ,$$

$$P(n,\delta) \approx \frac{n_{\rm sat}}{3} (1+3x)^2 \left[K_{\rm sat} x + \frac{1}{2} Q_{\rm sat} x^2 + \delta^2 \left(L_{\rm sym} + K_{\rm sym} x + \frac{1}{2} Q_{\rm sym} x^2 \right) \right] .$$

- $n < n_{sat}$

5.6. Empirical parameters

Isoscalar parameters

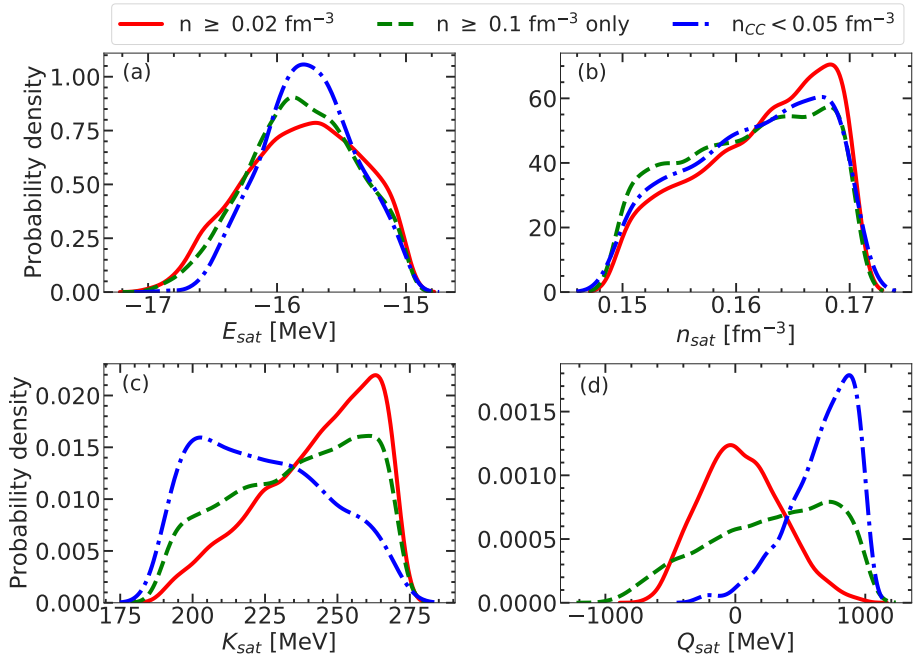

Isovector parameters

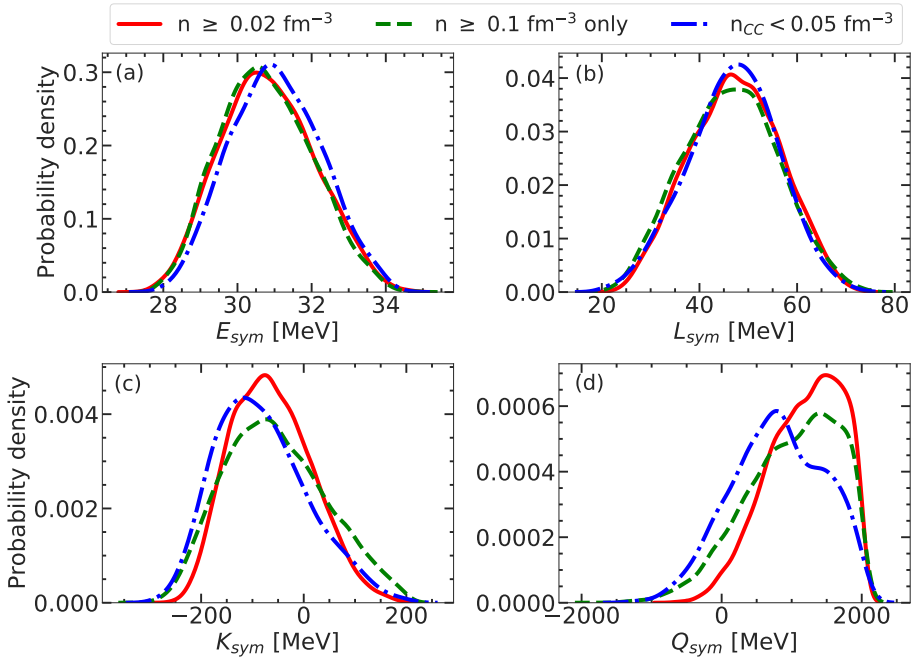

- Taylor expansions ($x = \dfrac{n - n_{sat}}{3n_{sat}}$, where $n_{sat} \approx 0.15$ fm^{-3}):

$$e(n,\delta) \approx E_{\rm sat} + \frac{1}{2} K_{\rm sat} x^2 + \frac{1}{6} Q_{\rm sat} x^3 + \delta^2 \left(E_{\rm sym} + L_{\rm sym} x + \frac{1}{2} K_{\rm sym} x^2 + \frac{1}{6} Q_{\rm sym} x^3 \right) ,$$

$$P(n,\delta) \approx \frac{n_{\rm sat}}{3} (1+3x)^2 \left[K_{\rm sat} x + \frac{1}{2} Q_{\rm sat} x^2 + \delta^2 \left(L_{\rm sym} + K_{\rm sym} x + \frac{1}{2} Q_{\rm sym} x^2 \right) \right] .$$

- $n < n_{sat} \rightarrow x < 0$

5.6. Empirical parameters

Isoscalar parameters | **Isovector parameters**

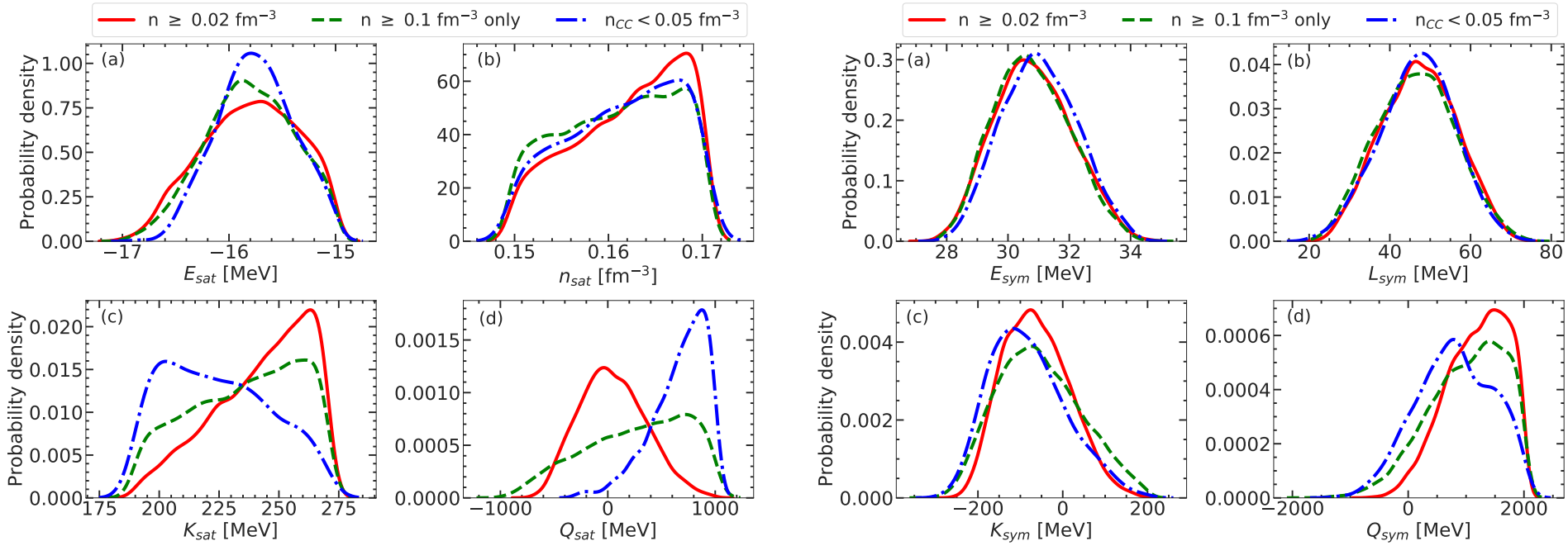

- Taylor expansions ($x = \dfrac{n - n_{sat}}{3n_{sat}}$, where $n_{sat} \approx 0.15$ fm^{-3}):

$$e(n,\delta) \approx E_{\rm sat} + \frac{1}{2} K_{\rm sat} x^2 + \frac{1}{6} Q_{\rm sat} x^3 + \delta^2 \left(E_{\rm sym} + L_{\rm sym} x + \frac{1}{2} K_{\rm sym} x^2 + \frac{1}{6} Q_{\rm sym} x^3 \right),$$

$$P(n,\delta) \approx \frac{n_{\rm sat}}{3} (1+3x)^2 \left[K_{\rm sat} x + \frac{1}{2} Q_{\rm sat} x^2 + \delta^2 \left(L_{\rm sym} + K_{\rm sym} x + \frac{1}{2} Q_{\rm sym} x^2 \right) \right].$$

- $n < n_{sat} \rightarrow x < 0 \rightarrow$ lower K_{sat} and higher Q_{sat} lead to lower energy and stiffer EoS.

5.7. Correlations

n_p

	E_{sat}	n_{sat}	K_{sat}	Q_{sat}	Z_{sat}	E_{sym}	L_{sym}	K_{sym}	Q_{sym}	Z_{sym}	σ_0	b_s	σ_{0c}	β	p
LD+HD ($n \geq 0.02$ fm^{-3})	-0.86	0.20	0.32	-0.27	0.02	0.32	-0.20	-0.25	0.22	-0.00	0.87	0.08	-0.73	-0.84	-0.09
LD+HD ($n \geq 0.1$ fm^{-3})	-0.44	0.03	0.39	-0.42	0.14	0.18	-0.19	-0.40	0.45	-0.14	0.44	0.02	-0.36	-0.47	-0.04
Prior	-0.28	0.01	0.09	-0.11	0.03	-0.04	0.06	-0.49	0.44	-0.06	0.29	0.06	-0.26	-0.22	-0.04

n_{CC}

	E_{sat}	n_{sat}	K_{sat}	Q_{sat}	Z_{sat}	E_{sym}	L_{sym}	K_{sym}	Q_{sym}	Z_{sym}	σ_0	b_s	σ_{0c}	β	p
LD+HD ($n \geq 0.02$ fm^{-3})	-0.04	-0.07	0.11	-0.05	-0.02	-0.30	-0.57	-0.15	0.45	-0.15	0.05	0.52	-0.15	-0.04	0.51
LD+HD ($n \geq 0.1$ fm^{-3})	-0.06	-0.06	0.33	-0.46	0.17	-0.15	-0.29	-0.10	0.39	-0.16	0.06	0.34	-0.11	-0.08	0.33
Prior	0.14	0.09	0.13	-0.18	0.02	0.08	-0.56	0.11	0.20	-0.05	-0.17	0.07	0.29	0.18	0.18

- Sphere-pasta transition density: isoscalar bulk (E_{sat}) and surface (σ_0, $\sigma_{0,c}$, β) are most influential.
- Crust-core transition density: isovector bulk (L_{sym}) and surface (b_s, p) parameters are most influential.

6. Conclusions

- Properties of the pasta phase are strongly model dependent.

6. Conclusions

- Properties of the pasta phase are strongly model dependent.
- The low-density part of the chiral EFT calculation is crucial in determining the pasta properties.

6. Conclusions

- Properties of the pasta phase are strongly model dependent.
- The low-density part of the chiral EFT calculation is crucial in determining the pasta properties.
- Apart from the bulk parameters, surface parameters are also influential in the determination of pasta properties.

BACKUP SLIDES

Surface parameters

- Mass of a spherical nucleus of charge Z and mass number A in vacuum:

$$M(A,Z)c^2 = m_p c^2 Z + m_n c^2 (A-Z) + \underbrace{A e_{HM}(n_0, I}_{\text{bulk energy}} + \underbrace{4\pi r_N^2 \left(\sigma_s + \frac{2\sigma_c}{r_N}\right)}_{\text{surface + curvature energies}} + \underbrace{\frac{3}{5}\frac{e^2 Z^2}{r_N}}_{\text{Coulomb energy}}$$

- Surface and curvature tensions depend on 5 surface parameters:

$$\sigma_s = \sigma_0 \frac{2^{p+1} + b_s}{y_p^{-p} + b_s + (1-y_p)^{-p}}$$

$$\sigma_c = 5.5\,\sigma_s \frac{\sigma_{0,c}}{\sigma_0}(\beta - y_p)\,,$$

- The 5 surface parameters are obtained by fitting $M(A,Z)$ to experimental nuclear mass table.

Shape dependence

- Expressions of surface, curvature, and Coulomb energy densities:

$$\epsilon_{surf} = \frac{ud\sigma_s}{r_n}, \tag{1}$$

$$\epsilon_{curv} = \frac{ud(d-1)\sigma_c}{r_n^2}, \tag{2}$$

$$\epsilon_{Coul} = 2\pi(eY_p n_0 r_n)^2 u \eta_{Coul,d}(u). \tag{3}$$

Uncertainties in surface and curvature tensions

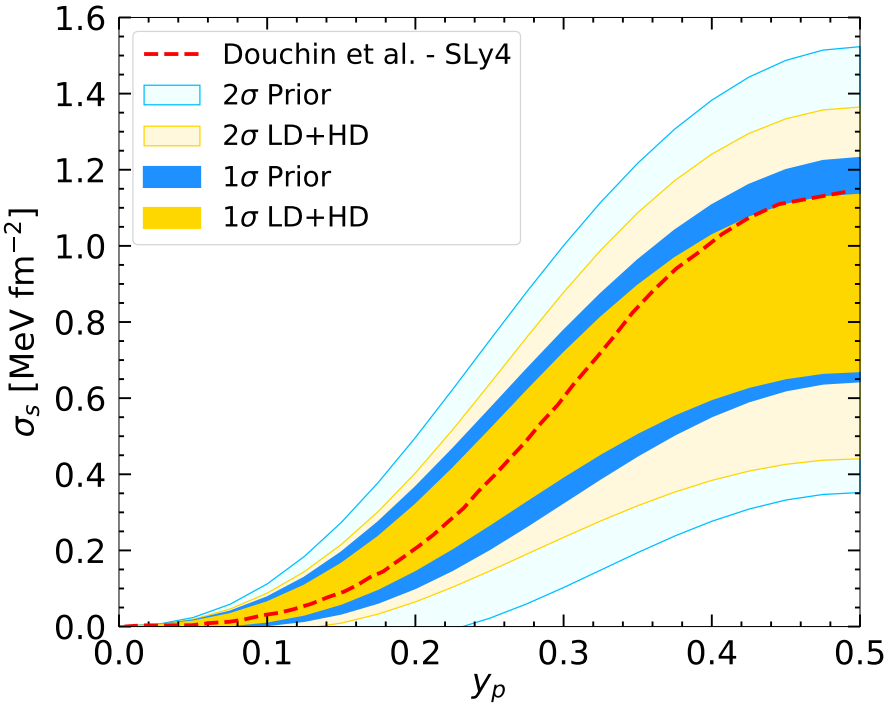

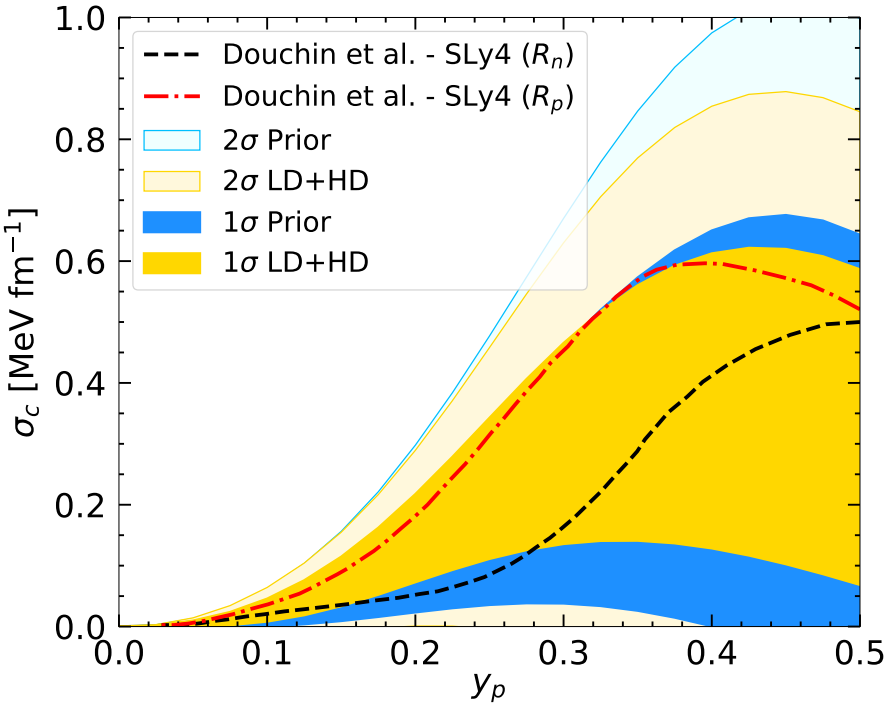

- Absolute uncertainties in surface and curvature tensions decrease with increasing proton fraction.
- Relative uncertainties in surface and curvature tensions increase with increasing proton fraction.
- The posteriors encompass the results from Douchin et al. 2000 for the SLy4 functional.

Fixing surface parameters

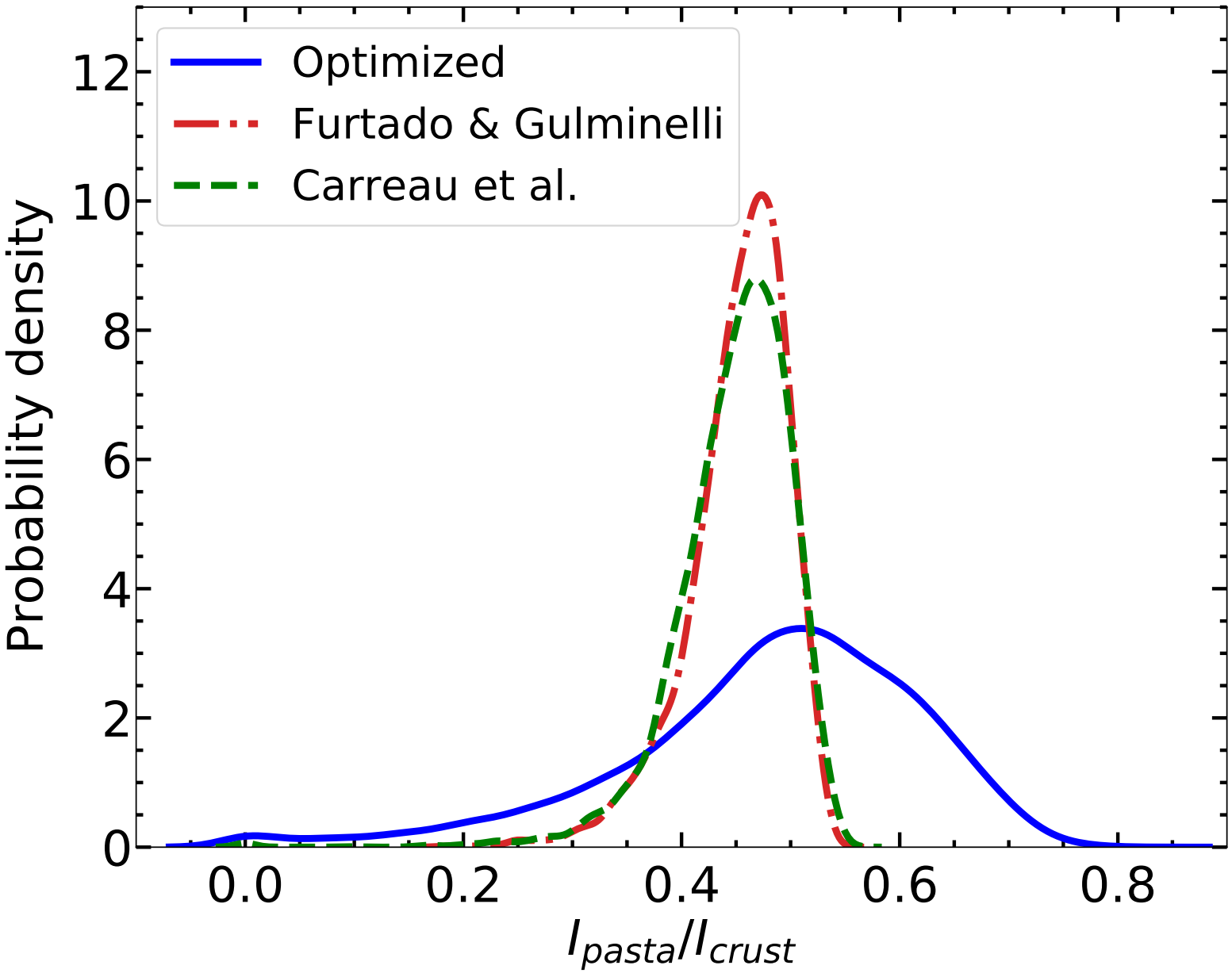

Nuclear matter energy

Dinh Thi, H., et al. . Eur. Phys. J. A 57, 296 (2021)

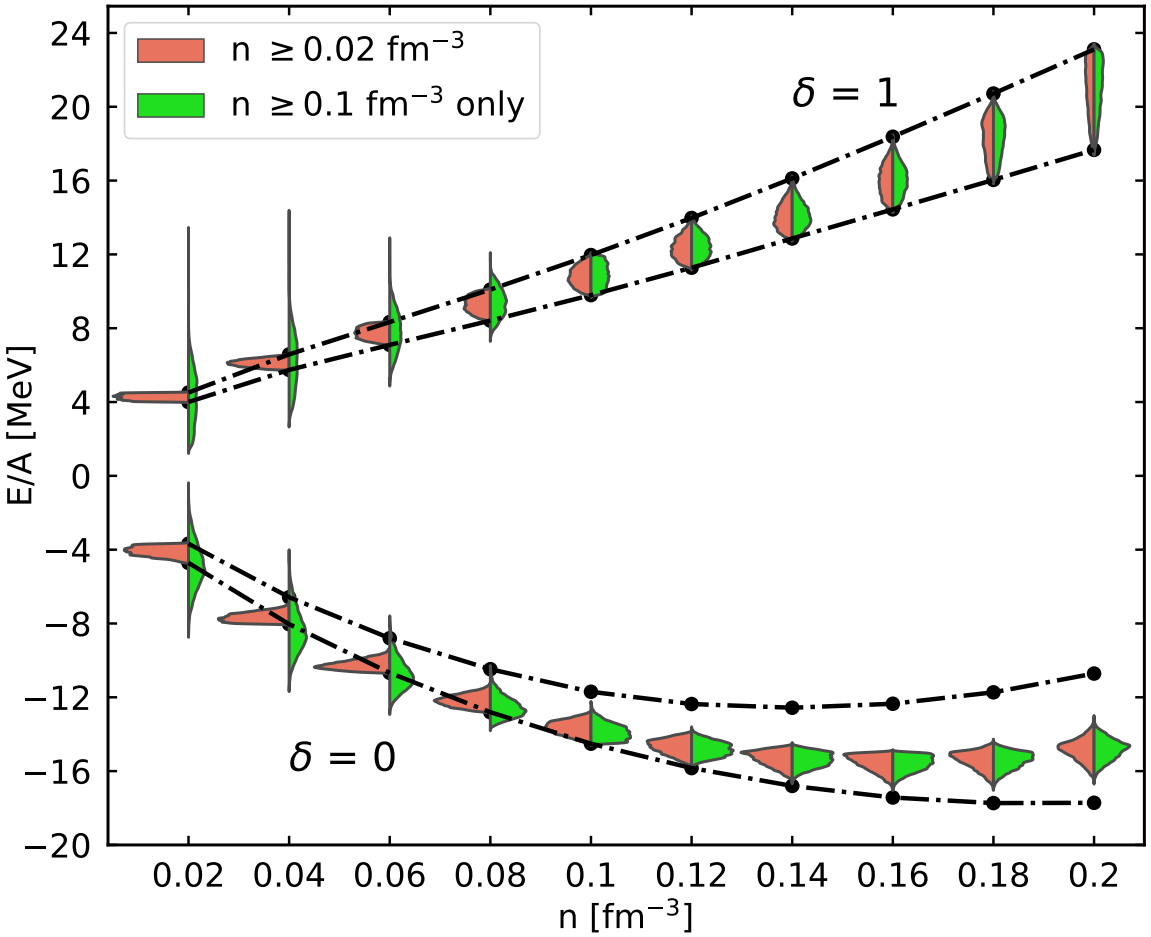

Prior distribution

Parameters	Min	Max
E_{sat} (MeV)	-17	-15
n_{sat} (fm^{-3})	0.15	0.17
K_{sat} (MeV)	190	270
Q_{sat} (MeV)	-1000	1000
Z_{sat} (MeV)	-3000	3000
E_{sym} (MeV)	26	38
L_{sym} (MeV)	10	80
K_{sym} (MeV)	-400	200
Q_{sym} (MeV)	-2000	2000
Z_{sym} (MeV)	-5000	5000
$m*_{sat}$	0.6	0.8
$\Delta m *_{sat} /m$	0.0	0.2
b	1	6